THE JOURNAL OF PROSTHETIC DENTISTRY

CLINICAL RESEARCH

Effect of the CBCT data segmentation threshold on registration accuracy with surface scanning

Lucio Lo Russo, DDS, PhD,[a] Mauro Lorusso, DDS,[b] Carlo Ercoli, DDS, PhD,[c] Roberto Sorrentino, DDS, PhD,[d] Domenico Ciavarella, DDS, PhD,[e] Gennaro Ruggiero, DDS, PhD,[f] and Fariba Esperouz, DDS[g]

ABSTRACT

Statement of problem. Accurate spatial relationships between cone beam computed tomography (CBCT) and intraoral surface scan (IOS) data is crucial to avoid encoding errors that can affect surgical and prosthetic planning, including surgical guide fabrication. Specifically, segmentation thresholds used during CBCT data processing may influence the geometry of 3D bone models and, consequently, the accuracy of their registration with the IOS data.

Purpose. The purpose of this study was to assess whether different CBCT segmentation thresholds affected the registration accuracy with IOSs.

Material and methods. CBCT and IOS data from 19 patients were included in the study. Standard tessellation language (STL) models were generated from CBCT scans using 7 segmentation thresholds (250–1750 HU). IOSs were aligned onto each bone model, and deviations were measured by using a metrology software program along the X-, Y-, and Z-axes at 6 reference points. The effect of thresholds, arch type, tooth type, and side was analyzed using generalized estimated equation (GEE) models (α=.05).

Results. A total of 231 models and 1306 measurements were obtained. The segmentation threshold significantly affected registration accuracy (*P*<.001 for all axes). The overall deviation ranged from −0.08 to 0.33 mm for the X-axis (anteroposterior direction), 0.01 to 0.03 mm for the Y-axis (left to right direction), and −0.13 to −0.66 mm for the Z-axis (apicocoronal direction). Measured deviations were consistent across arches and sides. In situations where a significant difference in Z-axis deviation was detected, irrespective of the segmentation threshold pair, the magnitude of this difference increased with higher segmentation thresholds.

Conclusions. Segmentation threshold in CBCT data processing significantly impacted the registration of IOSs to STL bone models, particularly in the apicocoronal direction. This may result in errors transferred to subsequent surgical and prosthetic phases, including surgical guide fabrication, thereby affecting implant positioning. Clinicians should be aware of this source of inaccuracy and consider it during planning. (J Prosthet Dent 2026;135:595.e1-e10)

Guided implant surgery has been demonstrated to enhance surgical efficiency and predictability and to decrease postoperative complications.[1] Guided surgery requires accurate preoperative prosthetic and surgical planning, which includes regional anatomy variability and safety during surgery.[2] A key factor in surgical planning is the visualization of the intended restoration in relation to the underlying soft and hard tissues[3] so that the implant position can be planned in the digital environment at the adequate maxillomandibular relationships and transferred to the surgical field by means of a surgical guide.[4–7]

Two sets of high-quality data, cone beam computed tomography (CBCT) and intraoral surface scans (IOSs),

This research did not receive any specific grant from funding agencies in the public, commercial, or not-for-profit sectors.
The authors declare that they have no known competing financial interests or personal relationships that could have appeared to influence the work reported in this paper.

[a]Professor of Prosthodontics, Department of Clinical and Experimental Medicine, School of Dentistry, University of Foggia, Foggia, Italy.
[b]PhD student, Department of Clinical and Experimental Medicine, School of Dentistry, University of Foggia, Foggia, Italy.
[c]Chairperson of Prosthodontics, Departments of Prosthodontics and Periodontics, Eastman Institute for Oral Health, University of Rochester, Rochester, NY.
[d]Professor of Prosthodontics, Department of Neurosciences, Reproductive and Odontostomatological Sciences, Scientific Unit of Digital Dentistry, University "Federico II" of Naples, Naples, Italy.
[e]Professor of Orthodontics, Department of Clinical and Experimental Sciences, University of Foggia, Foggia, Italy.
[f]Resident, Department of Neurosciences, Reproductive and Odontostomatological Sciences, Scientific Unit of Digital Dentistry, University "Federico II" of Naples, Naples, Italy.
[g]PhD student, Department of Clinical and Experimental Medicine, School of Dentistry, University of Foggia, Foggia, Italy.

Clinical Implications

CBCT segmentation thresholds play a critical role in determining the accuracy of IOS registration with bone models. Lack of consistency in the applied thresholds may result in positional errors during implant placement. Standardization is recommended to minimize errors.

need therefore to be properly merged and registered onto each other through common landmarks to ensure the correct relationship between their surface anatomies, and, as a function of that, correct relationships between prosthetic and surgical plans and auxiliary surgical devices such as surgical guides.[5,8–10]

IOSs of the edentulous arches are captured and stored in a standard tessellation language (STL) file format. The accuracy of IOSs has been well documented, with trueness and precision typically within 50 to 100 μm.[11] However, anatomic conditions have been reported to influence performance: dentate arches offer multiple landmarks that improve registration, while partially dentate and edentulous arches, with fewer reference points, may show reduced accuracy.[12,13] Digital imaging technologies have been primarily based on CBCT, which has been widely used in dentistry for implant surgery planning, or on multidetector computed tomography (MDCT).[14] Both of these technologies store data in the Digital Imaging and Communication in Medicine (DICOM) format.[15] The quality of imaging data may vary depending on the technology: device and operational parameters (such as, tube voltage, tube current, field of view (FOV), and voxel size).[16] However, in the case of CBCT, each voxel in a volumetric data set is assigned a gray value according to its radiation attenuation.[17] Voxel size and Hounsfield unit (HU) thresholds may also affect the accuracy of volumetric measurements.[18] Artifacts increase with voxel size and, therefore, optimal HU thresholds corresponding to different voxel sizes[16] should be considered. Furthermore, to be registered with the surface scan, DICOM voxel data need to be transformed into STL format,[19] thus providing a 3-dimensional (3D) geometry for alignment. Segmenting DICOM data is essential for generating 3D geometry.[20] The selected threshold determines which voxels are included and may affect the accuracy of bone, teeth, or other reference models used for alignment with surface data.[21,22] This may affect surgical and prosthetic planning and, more specifically, surgical guide fabrication. Indeed, since surgical guides are designed on surface anatomy, a lack of congruence between the planned position of implants and their actual position may result if segmentation thresholds affect the surface geometry of DICOM data. Although this may have significant implications for clinical and patient safety, data in this area are scarce.[5,23]

Guided implant surgery can simplify implant placement procedures, with increased safety and treatment delivery efficiency and improved clinical results.[24] For this to be possible, an accurate evaluation of the implant bone foundation is required to define an adequate implant position to ensure surgical safety and optimal prosthetic support. Such a planned implant position is obtained during surgery by means of a surgical guide. The surgical guide incorporates all the information necessary to transfer the planned implant position to the patient at the time of surgery; it is designed to fit the intraoral structures (teeth and/or mucosa) during surgery. If the position of the IOSs is not precisely matched to the underlying bone foundation (obtained from CBCT data), the implant position incorporated into the surgical guide may be inaccurate. Thus, the accurate matching of IOSs to the bone data is a critical step, which can be affected by the radiological data segmentation threshold, that is, the HU threshold selected to obtain the 3D bone model to be used for alignment with the IOSs.

Therefore, the objective of this study was to evaluate how the segmentation threshold of DICOM data may affect the dimensional accuracy of 3D models and, consequently, the alignment with surface scans. The null hypothesis was that the segmentation threshold would have no significant effect on the dimensional accuracy of 3D models obtained by using the CBCT data.

MATERIAL AND METHODS

Data from 19 patients previously treated with implant-supported prosthetic rehabilitation were retrospectively retrieved from electronic records, with ethics approval. The study workflow is summarized in Figure 1. For each patient, DICOM and intraoral surface datasets were obtained by means of CBCT (Orthophos XG3D; Dentsply Sirona) and intraoral scans (TRIOS 4; 3Shape A/S).

The DICOM data were imported into a software program (Blue Sky Plan 4; Blue Sky Bio, LLC), and STL models of the maxillary and mandibular arches were obtained by using different segmentation thresholds. Specifically, 7 different HU values (250, 500, 750, 1000, 1250, 1500, 1750) were selected as thresholds for segmentation. As a function of these thresholds, voxels with HU values above each such threshold were incorporated into the corresponding STL models (Figs. 2, 3). For each arch of each patient, 7 STL models were obtained and numbered from RX1 (corresponding to model obtained with the 250 HU segmentation threshold) to RX7 (corresponding to 1750 HU).

Once exported, the RX1 to RX7 models were further processed (Geomagic Wrap 2024; 3D Systems Inc), where their position was aligned along the following directions

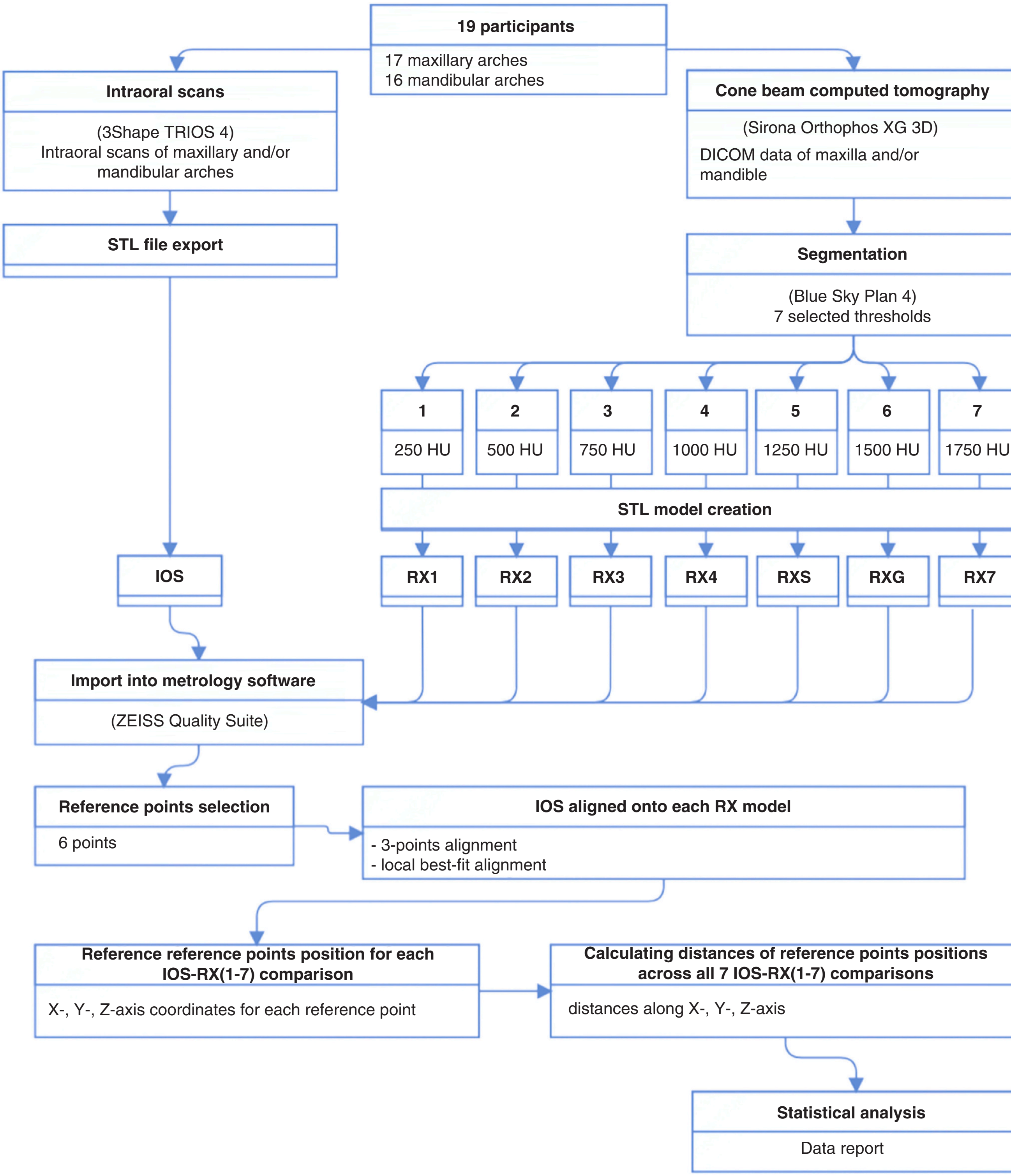

Figure 1. Flowchart of study protocol.

of the global coordinates system: anteroposterior direction (sagittal plane) along the X-axis, left to right direction (frontal plane) along the Y-axis, and apicocoronal direction (axial plane) along the Z-axis.

Misalignment between IOSs and each RX model was measured by importing their STL files into a software program (GOM Inspect Pro ZEISS Quality Suite). The methodology was first described for the comparison of

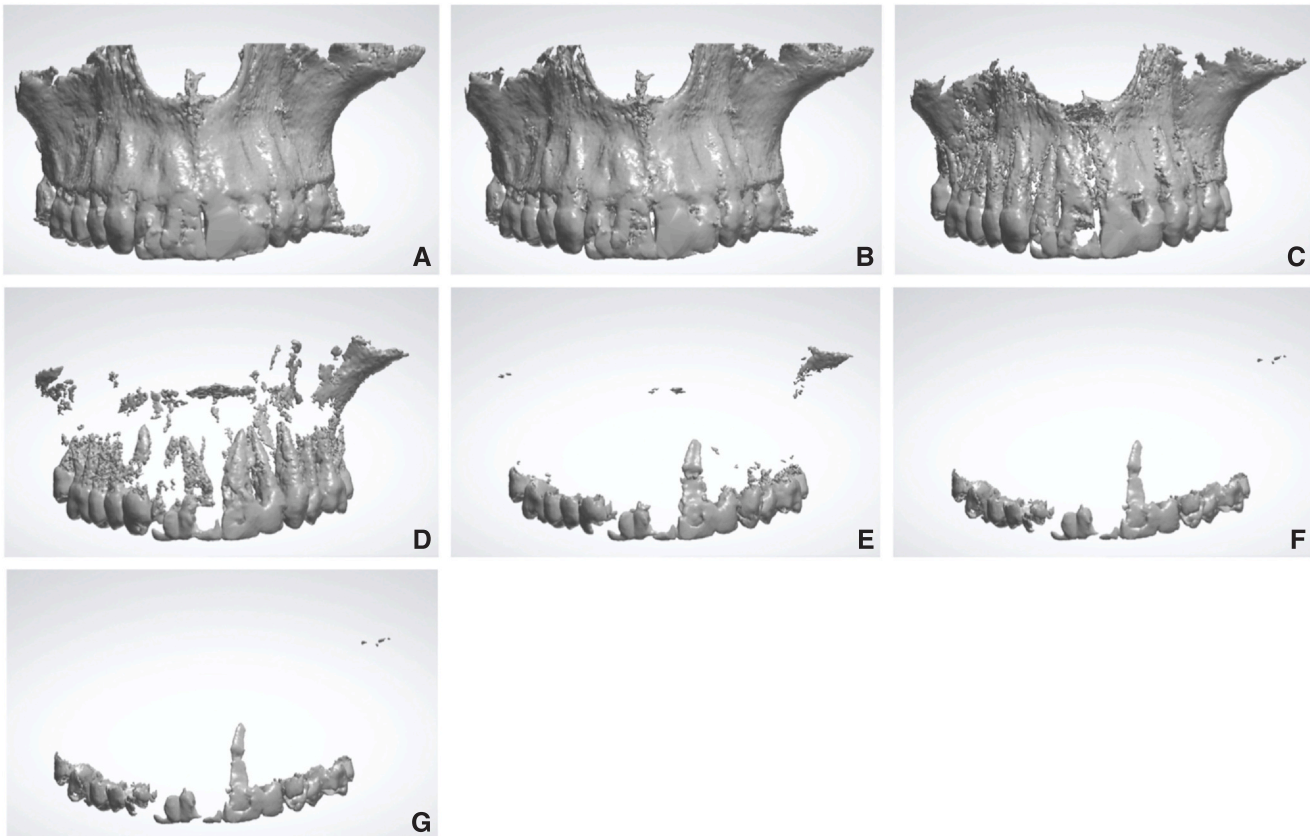

Figure 2. Three-dimensional models of maxillary arch created in 1 investigated individual by using 7 segmentation thresholds. A, 250 HU. B, 500 HU. C, 750 HU. D, 1000 HU. E, 1250 HU. F, 1500 HU. G, 1750 HU.

RX1 and IOSs and was subsequently repeated for the remaining RX2 to RX7 models.

Six reference points for measurements were selected on each IOS: the mesiobuccal cusp of the first molar (M), the canine cusp (C), and the middle of the incisal edge of the central incisor (I) on both the left and the right side (Fig. 4A, B). The coordinates of such points were recorded to ensure consistency and standardization across comparisons.

An initial alignment between RX1 and IOSs was performed by using a 3-point alignment method and with RX1 as the reference (Fig. 5); subsequently, the alignment was fined tuned by means of a local best-fit and considering teeth as the area of interest. For the 3-point alignment method, the mesiobuccal cusp of the first molar, the cusp tip of the canine, and the middle of the incisal edge of the central incisor were selected as reference points. The same 3 points were consistently applied to all models to ensure standardization across situations. A color difference map was also obtained for visualization and analysis of the deviation pattern for both the maxillary and mandibular arches (Fig. 6).

After the alignment, the X-, Y-, Z-coordinates of the reference points were recorded in a standardized data registration form. Thus, after the alignment of the IOSs onto each RX1 to RX7 model, 7 datasets were obtained and compared. The outcome of interest was the potential alignment deviation related to the RX models obtained with the 7 segmentation thresholds (Fig. 7). The null hypothesis was made under the assumption that if the segmentation thresholds had no effect on the dimensional accuracy of the STL file of the bone structure, the alignment of IOSs onto them would always be the same and the distance between the reference points would be zero.

Such distances were obtained from calculations using their coordinates and detailed for the X-, Y-, and Z-axis; the position of reference points in the comparison including RX1 (such as the model obtained selecting the lowest segmentation threshold) was considered as reference; in other words, the distances were calculated by subtracting the coordinates of each point from the corresponding reference point in the RX1–IOS alignment. Thus, for each segmentation threshold, each of the 6 reference points was annotated with information regarding the X-, Y-, and Z-axis distance relative to the RX1 position, the arch type, the tooth type, and the side.

The effects of measurement positions, between and within models obtained with the selected segmentation thresholds, on deviations along the X-, Y-, and Z-axes

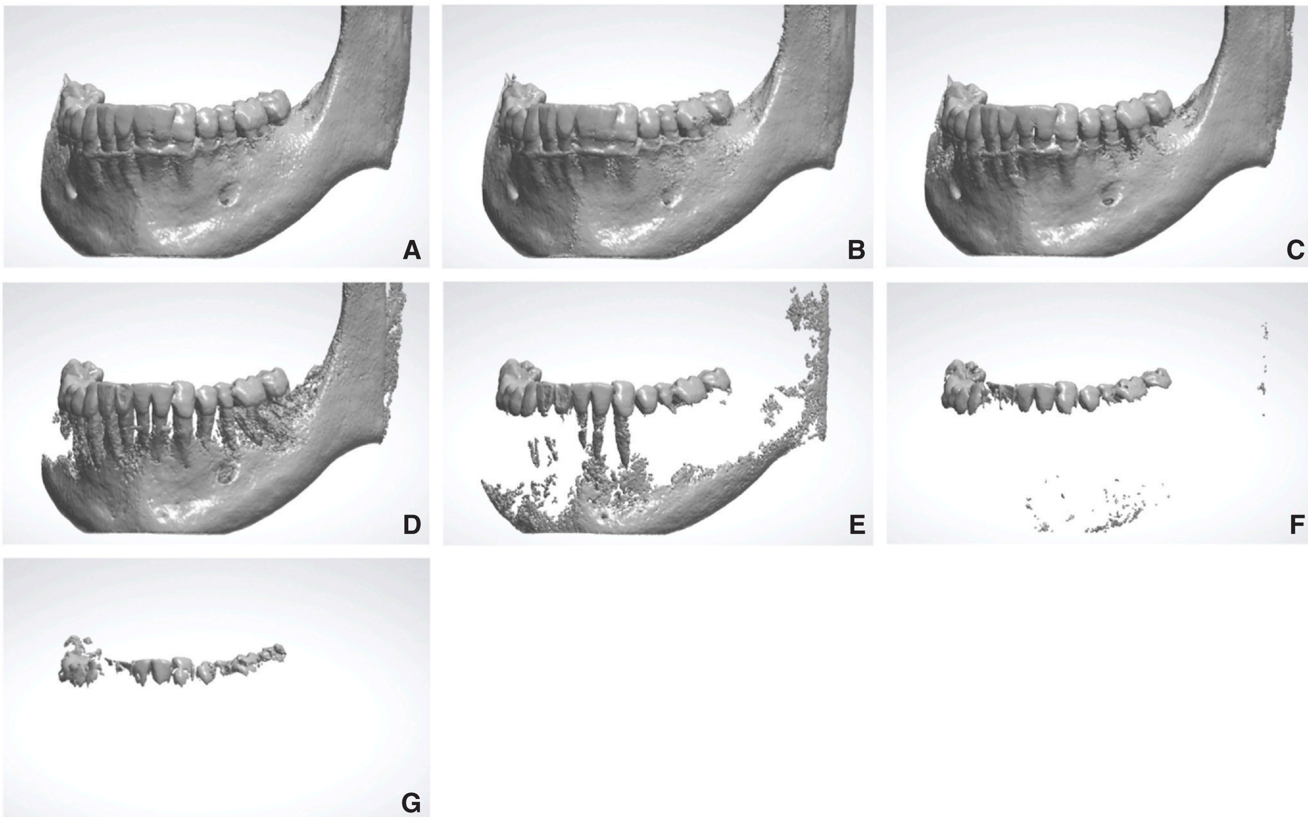

Figure 3. Three-dimensional models of mandibular arch created in 1 investigated individual by using 7 segmentation thresholds. A, 250 HU. B, 500 HU. C, 750 HU. D, 1000 HU. E, 1250 HU. F, 1500 HU. G, 1750 HU.

were also investigated by using generalized estimated equation (GEE) models. The GEE methodology was used to model and control the within-unit measurements from the 6 locations. The patient was used as a subject-variable; segmentation thresholds (1: 250 HU; 2: 500 HU; 3: 750 HU; 4: 1000 HU; 5: 1250 HU; 6: 1500 HU; 7: 1750 HU), arch type (maxillary or mandibular), tooth type (M, C, I), and side (right or left) were included as factors to investigate differences measured along each axis, while the variations of the remaining 2 axes were included as covariates. In addition, the nested effect of these factors was considered in the model. The analysis was performed with a statistical software program (IBM SPSS Statistics, v25.0; IBM Corp) (α=.05).

RESULTS

From the 19 participants enrolled in the study, data from 17 maxillary and 16 mandibular arches were available. According to the study methodology, 231 STL models were therefore obtained from the CBCT (119 maxillary,

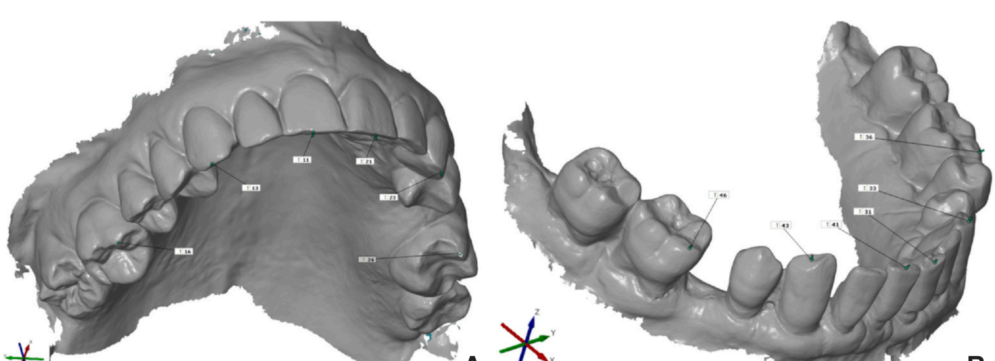

Figure 4. Reference points for measurements selected on each scan: mesiobuccal cusp of first molar (M), canine cusp (C), and middle of incisal edge of central incisor (I) on both left and right side. Note position of models in relation to coordinate system. A, Maxillary arch. B, Mandibular arch.

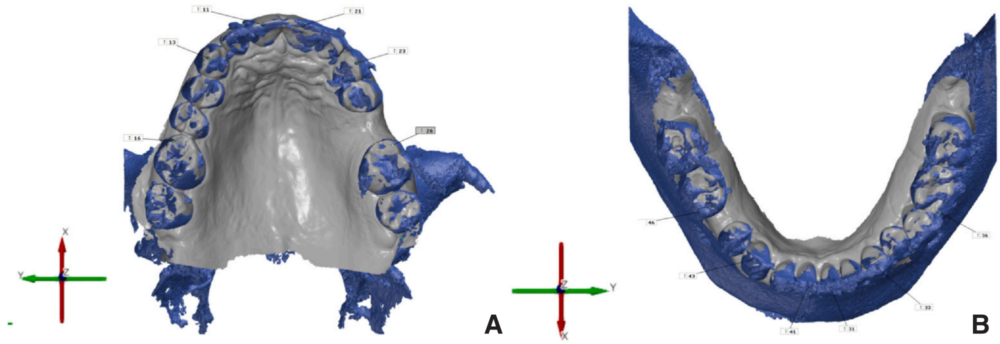

Figure 5. Initial alignment between RX1 models and intraoral scan by using three-point alignment method and taking RX1 as reference.

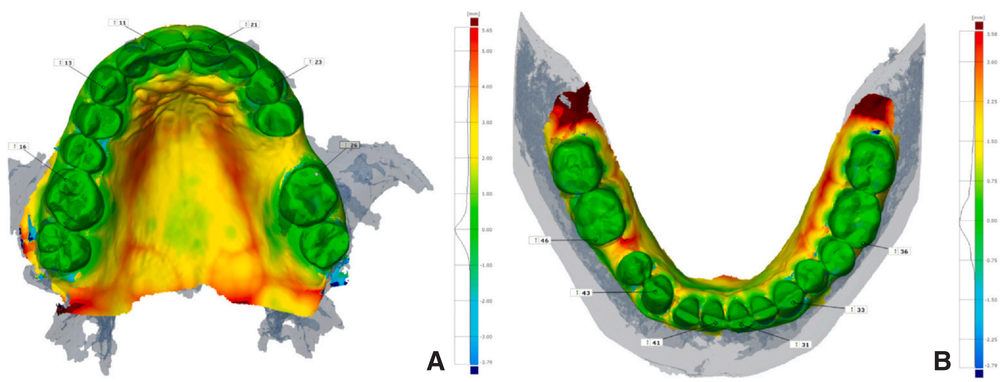

Figure 6. Color difference map obtained for visualization and analysis of deviation pattern after tuning alignment by using local best-fit on teeth surface. A, Maxillary arch. B, Mandibular arch.

112 mandibular). A total of 1306 measurements on the corresponding reference points were made. The distance between such reference points was measured and detailed on the X-, Y- and Z- axis. The estimated marginal means of such measurements, as obtained from the GEE models and detailed for each segmentation threshold, are shown in Table 1. The overall deviation ranged from −0.08 to 0.33 mm for the X-axis, 0.01 to 0.03 mm for the Y-axis, and −0.13 to −0.66 mm for the Z-axis. The greatest deviation was observed for the Z-axis and progressively increased from RX1 to RX7. The minus sign indicates that the greater the segmentation threshold, the more the IOS is positioned in a more apical position onto the corresponding RX model. The GEE models showed significant effects of the segmentation threshold either alone or in combination with tooth type; the combined effect of segmentation threshold with arch and side was significant for the X-axis and Y-Axis, respectively (Table 2).

In Table 3 the deviations measured at reference points across positions of IOSs aligned onto RX models were stratified according to arch, tooth type, and side factors. The pairwise comparison of estimated marginal means of dependent variables (X-, Y-, Z-axis deviations)

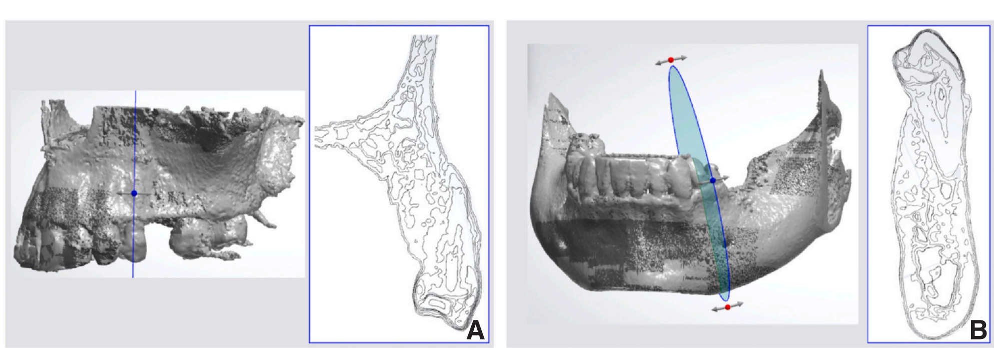

Figure 7. Modifications of RX models because of segmentation thresholds. Cross section made across all superimposed 7 RX models shows differences in external boundary and anatomic shape; deviations evident on tooth surface. A, Maxillary arch. B, Mandibular arch.

Table 1. Deviation (mm) measured at reference points across positions of IOSs aligned onto RX models obtained with different segmentation thresholds; measurements obtained considering RX1 (model made by means of lowest segmentation threshold (250 HU)) as reference

		Segmentation Threshold						
		1	2	3	4	5	6	7
X-axis	Mean	0.00	0.11	0.07	0.33	0.06	−0.03	−0.08
	S.E.	0.00	0.11	0.09	0.35	0.12	0.06	0.06
	95% C.I. Lower	0.00	−0.11	−0.11	−0.35	−0.19	−0.16	0.19
	95% C.I. Upper	0.00	0.33	0.26	1.02	0.30	0.09	0.04
Y-axis	Mean	0.00	0.01	0.02	0.03	0.02	0.02	0.01
	S.E.	0.00	0.01	0.02	0.02	0.02	0.02	0.02
	95% C.I. Lower	0.00	−0.01	−0.02	−0.02	−0.03	−0.02	−0.03
	95% C.I. Upper	0.00	0.03	0.07	0.07	0.06	0.06	0.06
Z-axis	Mean	0.00	−0.13	−0.27	−0.39	−0.49	−0.58	−0.66
	S.E.	0.00	0.01	0.01	0.01	0.02	0.03	0.03
	95% C.I. Lower	0.00	−0.14	−0.29	−0.42	−0.53	−0.63	−0.72
	95% C.I. Upper	0.00	−0.11	−0.25	−0.36	−0.45	−0.53	−0.59

C.I., confidence interval; S.E., standard error.

Table 2. Results from generalized estimated equation models addressing effects of investigated factors on deviation measured at reference points

	P		
Factors	**X-Axis**	**Y-Axis**	**Z-Axis**
Intercept	.502	.366	**<.001**
SEGMENTATION THRESHOLD	**<.001**	**.003**	**<.001**
ARCH	.382	.429	.095
TOOTH	.399	.325	.116
SIDE	.317	.303	.708
Threshold*arch	**.001**	.277	.080
Threshold*tooth	**<.001**	**.003**	**<.001**
Threshold*side	.065	**.001**	.085

Bold: statistically significant (*P*<.05).

(Table 4), according to such factors, showed no significance for differences between maxillary and mandibular arch, or for left and right side. As regards tooth type, a significant difference was found only for the Z-axis deviation between canine and incisor. Differences were always significant for Z-axis deviations across all segmentation thresholds. Some significant differences were also found for the X-, and Y-axis, but with no evident pattern. However, a clear pattern was seen for the Z-axis. Significant differences in Z-axis deviation were present for all segmentation threshold pairs, with differences increasing as the HU threshold increased (0.13 to 0.66 mm from RX1 to RX7).

DISCUSSION

In the present study it was observed that the segmentation threshold may cause distortion of RX models; this, in turn, may cause deviations (Table 1), which were found to be statistically significant, in the position of IOSs aligned onto them along the X-axis, Y-axis, Z-axis (*P*<.001, *P*=.003, *P*<.001, respectively) (Table 2). Thus, the null hypothesis that the segmentation threshold would have no significant effects on the dimensional accuracy of 3D models obtained using the CBCT data was rejected.

The measured deviations related to segmentation thresholds were consistent and not significant between arches. In fact, the "arch" factor had no significant effect on the deviations of reference points, as shown by GEE models (X-axis: *P*=.382; Y-axis: *P*=.429; Z-axis: *P*=.095), and the mean differences between the maxillary and mandibular arches (X-axis: −0.24 mm; Y-axis: 0.01 mm; Z-axis: 0.03 mm) were not significant (*P*>.05) (Table 4).

Within each arch, deviations were measured at 6 reference points distributed along the arch and identified by specific dental landmarks. This distribution allowed the capture of positional information of the entire arch within the coordinate system. The position of measurements within the arch (like the "tooth" factor) had no significant effect on deviations measured at reference points (X-axis: *P*=.399; Y-axis: *P*=.325; Z-axis: *P*=.116). Only the mean difference on the Z-axis (0.01 mm) between canine and incisor were statistically significant (*P*=.043).

Similarly, measured deviations were consistent between left and right side. The "side" factor had no significant effect (X-axis: *P*=.317; Y-axis: *P*=.303; Z-axis: *P*<.001), and the mean differences between left and right side (X-axis: 0.06 mm; Y-axis: 0.00 mm; Z-axis: 0.00 mm) were not significant (*P*>.05).

Taken together, these observations suggested that the HU threshold selected during CBCT data segmentation may cause a significant deviation in the IOS position onto the RX model. This deviation was consistent between the maxillary and mandibular arch, as well as between the left and right sides. Along the Z-axis (apicocoronal direction),

Table 3. Deviation (mm) measured at reference points, stratified according to arch, tooth type, and side factors

Factors			Deviation		
			X-axis	Y-axis	Z-axis
Arch	Maxilla (MAX)	Mean	−0.03	0.02	−0.35
		S.E.	0.02	0.02	0.02
		95% C.I. Lower	−0.07	−0.03	−0.38
		95% C.I. Upper	0.01	0.07	−0.31
	Mandible (MND)	Mean	0.21	0.01	−0.37
		S.E.	0.27	0.01	0.01
		95% C.I. Lower	−0.32	−0.02	−0.40
		95% C.I. Upper	0.74	0.03	−0.34
Tooth	Molar (M)	Mean	0.40	0.03	−0.35
		S.E.	0.40	0.02	0.01
		95% C.I. Lower	−0.39	−0.02	−0.37
		95% C.I. Upper	1.18	0.07	−0.32
	Canine (C)	Mean	−0.07	0.01	−0.36
		S.E.	0.01	0.01	0.02
		95% C.I. Lower	−0.10	−0.02	−0.39
		95% C.I. Upper	−0.04	0.03	−0.33
	Incisor (I)	Mean	−0.06	0.01	−0.37
		S.E.	0.02	0.02	0.02
		95% C.I. Lower	−0.09	−0.03	−0.41
		95% C.I. Upper	−0.02	0.05	−0.34
Side	Right	Mean	0.12	0.01	−0.36
		S.E.	0.16	0.02	0.02
		95% C.I. Lower	−0.20	−0.02	−0.39
		95% C.I. Upper	0.44	0.05	−0.33
	Left	Mean	0.06	0.02	−0.36
		S.E.	0.11	0.02	0.01
		95% C.I. Lower	−0.15	−0.02	−0.38
		95% C.I. Upper	0.26	0.05	−0.33

C.I., confidence interval; S.E., standard error.

Table 4. Pairwise comparison of estimated marginal means (mm) of dependent variables form GEE models, and significance of their differences

Factors			X-axis			Y-axis			Z-axis		
	A	B	Mean Difference (A − B)	SE	*P*	Mean Difference (A − B)	SE	*P*	Mean Difference (A − B)	SE	*P*
ARCH	MAX	MND	−0.24	0.28	.382	0.01	0.02	.429	0.03	0.02	.095
TOOTH	C	I	−0.01	0.01	.274	−0.01	0.01	.456	0.01	0.01	**.043**
		M	−0.47	0.41	.250	−0.02	0.02	.138	−0.01	0.01	.351
	I	M	−0.45	0.40	.259	−0.02	0.01	.169	−0.02	0.01	.075
SIDE	Right	Left	0.06	0.06	.317	0.00	0.00	.303	0.00	0.01	.708
SEGMENTATION THRESHOLD	1	2	0.05	0.03	.132	−0.02	0.01	.159	0.13	0.01	**<.001**
		3	0.09	0.05	.086	−0.03	0.02	.201	0.27	0.01	**<.001**
		4	−0.18	0.21	.405	−0.03	0.03	.209	0.39	0.01	**<.001**
		5	0.10	0.02	**<.001**	−0.03	0.03	.316	0.49	0.02	**<.001**
		6	0.19	0.08	**.023**	−0.03	0.02	.265	0.58	0.02	**<.001**
		7	0.23	0.09	**.009**	−0.02	0.02	.386	0.66	0.03	**<.001**
	2	3	0.04	0.02	**.046**	−0.01	0.01	.269	0.14	0.01	**<.001**
		4	−0.22	0.24	.357	−0.02	0.01	.284	0.27	0.01	**<.001**
		5	0.06	0.02	**<.001**	−0.01	0.01	.537	0.36	0.02	**<.001**
		6	0.15	0.06	**.007**	−0.01	0.01	.477	0.45	0.02	**<.001**
		7	0.19	0.06	**.002**	−0.00	0.02	.751	0.53	0.03	**<.001**
	3	4	−0.26	0.26	.314	−0.00	0.00	.690	0.12	0.01	**<.001**
		5	0.02	0.03	.610	0.00	0.01	.393	0.22	0.01	**<.001**
		6	0.11	0.04	**.003**	0.00	0.01	.466	0.31	0.02	**<.001**
		7	0.15	0.04	**<.001**	0.01	0.01	.361	0.39	0.03	**<.001**
	4	5	0.28	0.23	.227	0.01	0.00	**.002**	0.10	0.01	**<.001**
		6	0.37	0.29	.209	0.01	0.00	.173	0.19	0.02	**<.001**
		7	0.41	0.30	.168	0.01	0.01	.166	0.27	0.02	**<.001**
	5	6	0.09	0.06	.157	0.00	0.00	.967	0.09	0.01	**<.001**
		7	0.13	0.07	.054	0.00	0.01	.526	0.17	0.02	**<.001**
	6	7	0.04	0.01	**<.001**	0.00	0.01	.559	0.08	0.01	**<.001**

C, canine; I, incisor; M, molar; SE, standard error.
Bold: statistically significant ($P<.05$).

a statistically significant deviation was found in a more apical direction ($P<.05$), progressively increasing (in an approximately linear function) from 0.13 mm (RX1) to 0.66 mm (RX7). This finding was similar to results from clinical data from Flugge et al[5] (0.54 mm) and Nkenke et al[25] (0.56 mm for the maxillary arch, 0.66 mm for the mandibular arch) investigating registration accuracy using tooth surface, although in the cited studies the deviation was reported without insights into its components along references axes.

The clinical implication was that while increasing the segmentation threshold, the IOSs were aligned onto the RX model in a more apical position (up to 0.66 mm). Therefore, the surgical guide designed on such IOSs would have the same position as the IOSs in relation to the bone foundation. Since in fully guided implant surgery, the surgical guide also defines the corono-apical stop of implant position, the above reported deviation (0.13 to 0.66 mm) may be transferred to the implant with different implications at the implant apex or implant platform.[26]

Deviation at the implant apex may affect surgical safety in terms of the protection of anatomic structures, whereas the deviation at the implant platform may affect the position of the implant-to-abutment interface in relation to the bone crest.

Given the order of magnitude of the reported deviation, the clinical significance of both surgical and prosthetic implications cannot be estimated and needs to be determined on a situation-by-situation basis. In addition, in the present study, measurements were performed relative to the lowest segmentation threshold: this was arbitrary and substantiated the potential methodological limitation because of the absence of an absolute threshold. Defining what is the "right" or the best threshold to use is not possible: this is a matter of correct visualization and the representation of anatomic structures and is highly dependent on the situation and operator and the presence of artifacts. The importance of manually selecting segmentation thresholds has already been highlighted because the default gray value range provided by the software program may compromise the display of anatomic structures and especially teeth.[5,27]

Additional limitations of the study could be related to the technologies and methodology used. Those planning and installing the implants contribute to the overall error in implant position as a result of their choice of segmentation threshold in imaging data processing because the reported potential implications require a balanced decision or appropriate actions.

CONCLUSIONS

Based on the findings of this study, the following conclusions were drawn:

1. CBCT segmentation thresholds significantly affected the registration accuracy of IOSs to 3D bone models, particularly along the Z-axis, where deviations increased progressively from 0.13 mm at the lowest threshold (250 HU) to 0.66 mm at the highest threshold (1750 HU).
2. These deviations, although consistent between arches and sides, may result in clinically relevant misalignments when designing and using surgical guides, with potential consequences for implant positioning.
3. Standardizing segmentation thresholds is therefore recommended to minimize errors during digital implant planning and guided surgery.

REFERENCES

1. D'Addazio G, Xhajanka E, Traini T, et al. Accuracy of DICOM-DICOM vs. DICOM-STL protocols in computer-guided surgery: A human clinical study. *J Clin Med*. 2022;11:2336.
2. Ganz SD. Three-dimensional imaging and guided surgery for dental implants. *Dent Clin North Am*. 2015;59:265–290.
3. Scherer MD. Presurgical implant-site assessment and restoratively driven digital planning. *Dent Clin North Am*. 2014;58:561–595.
4. Bornstein MM, Scarfe WC, Vaughn VM, Jacobs R. Cone beam computed tomography in implant dentistry: a systematic review focusing on guidelines, indications, and radiation dose risks. *Int J Oral Maxillofac Implants*. 2014;29:55–77.
5. Flügge T, Derksen W, Te Poel J, Hassan B, Nelson K, Wismeijer D. Registration of cone beam computed tomography data and intraoral surface scans - A prerequisite for guided implant surgery with CAD/CAM drilling guides. *Clin Oral Implants Res*. 2017;28:1113–1118.
6. Lo Russo L, Caradonna G, Troiano G, Salamini A, Guida L, Ciavarella D. Three-dimensional differences between intraoral scans and conventional impressions of edentulous jaws: A clinical study. *J Prosthet Dent*. 2020;123:264–268.
7. Mora MA, Chenin DL, Arce RM. Software tools and surgical guides in dental-implant-guided surgery. *Dent Clin North Am*. 2014;58:597–626.
8. Choi Y-S, Kim M-K, Lee J-W, Kang S-H. Impact of the number of registration points for replacement of three-dimensional computed tomography images in dental areas using three-dimensional light-scanned images of dental models. *Oral Radiology*. 2014;30:32–37.
9. Lin HH, Chiang WC, Lo LJ, Sheng-Pin Hsu S, Wang CH, Wan SY. Artifact-resistant superimposition of digital dental models and cone-beam computed tomography images. *J Oral Maxillofac Surg*. 2013;71:1933–1947.
10. Ritter L, Reiz SD, Rothamel D, et al. Registration accuracy of three-dimensional surface and cone beam computed tomography data for virtual implant planning. *Clin Oral Implants Res*. 2012;23:447–452.
11. Borbola D, Mikolicz A, Romanszky L, et al. Complete-arch accuracy of seven intraoral scanners measured by the virtual-fit method. *J Dent*. 2024;149:105281.
12. Lo Russo L, Sorrentino R, Esperouz F, Zarone F, Ercoli C, Guida L. Assessment of distortion of intraoral scans of edentulous mandibular arch made with a 2-step scanning strategy: A clinical study. *J Prosthet Dent*. 2025;134:151–159.
13. Srivastava G, Padhiary SK, Mohanty N, Molinero-Mourelle P, Chebib N. Accuracy of intraoral scanner for recording completely edentulous arches-A systematic review. *Dent J (Basel)*. 2023;11:241.
14. Scarfe WC, Farman AG. What is cone-beam CT and how does it work. *Dent Clin North Am*. 2008;52:707–730.
15. Burgess J. Digital DICOM in dentistry. *Open Dent J*. 2015;9:330–336.
16. Dong T, Xia L, Cai C, Yuan L, Ye N, Fang B. Accuracy of in vitro mandibular volumetric measurements from CBCT of different voxel sizes with different segmentation threshold settings. *BMC Oral Health*. 2019;19:206.
17. Kernen F, Kramer J, Wanner L, Wismeijer D, Nelson K, Flügge T. A review of virtual planning software for guided implant surgery - Data import and visualization, drill guide design and manufacturing. *BMC Oral Health*. 2020;20:251.
18. Mah P, Reeves TE, McDavid WD. Deriving Hounsfield units using grey levels in cone beam computed tomography. *Dentomaxillofac Radiol*. 2010;39:323–335.
19. Zhao XZ, Xu WH, Tang ZH, Wu MJ, Zhu J, Chen S. Accuracy of computer-guided implant surgery by a CAD/CAM and laser scanning technique. *Chin J Dent Res*. 2014;17:31–36.

20. Lo Presti G, Carbone M, Ciriaci D, Aramini D, Ferrari M, Ferrari V. Assessment of DICOM viewers capable of loading patient-specific 3D models obtained by different segmentation platforms in the operating room. *J Digit Imaging*. 2015;28:518–527.
21. Friedli L, Kloukos D, Kanavakis G, Halazonetis D, Gkantidis N. The effect of threshold level on bone segmentation of cranial base structures from CT and CBCT images. *Sci Rep*. 2020;10:7361.
22. Poleti ML, Fernandes TMF, Moretti MR, Puzinato LR, Slaviero TVS, Rubira-Bullen IRF. Reliability and accuracy of automatic segmentation of mandibular 3D models on linear measurements. *Clin Oral Investig*. 2021;25:6335–6346.
23. Tatakis DN, Chien HH, Parashis AO. Guided implant surgery risks and their prevention. *Periodontol 2000*. 2019;81:194–208.
24. Schneider D, Marquardt P, Zwahlen M, Jung RE. A systematic review on the accuracy and the clinical outcome of computer-guided template-based implant dentistry. *Clin Oral Implants Res*. 2009;20:73–86.
25. Nkenke E, Zachow S, Benz M, et al. Fusion of computed tomography data and optical 3D images of the dentition for streak artefact correction in the simulation of orthognathic surgery. *Dentomaxillofac Radiol*. 2004;33:226–232.
26. Lo Russo L, Ercoli C, Guida L, Merli M, Laino L. Surgical guides for dental implants: Measurement of the accuracy using a freeware metrology software program. *J Prosthodont Res*. 2023;67:300–304.
27. Swennen GR, Mollemans W, Schutyser F. Three-dimensional treatment planning of orthognathic surgery in the era of virtual imaging. *J Oral Maxillofac Surg*. 2009;67:2080–2092.

Corresponding author:
Dr Fariba Esperouz
School of Dentistry
University of Foggia
Via Luigi Rovelli, 50
Foggia, Puglia 71121
ITALY
Email: fariba.esperouz@unifg.it

https://doi.org/10.1016/j.prosdent.2025.10.044